Earthquakes and Structures, *Vol. 8, No. 5 (2015) 1069-1089*
DOI: http://dx.doi.org/10.12989/eas.2015.8.5.1069

Seismic response of non-structural components attached to reinforced concrete structures with different eccentricity ratios

Ayad B. Aldeka[*1], Samir Dirar[1a], Andrew H.C. Chan[2b] and Pedro Martinez-Vazquez[1c]

[1]*School of Civil Engineering, University of Birmingham, Edgbaston, Birmingham, B15 2TT, United Kingdom*
[2]*School of Science, Information Technology and Engineering (Ballarat), Federation University Australia, Victoria 3350, Australia*

(Received July 16, 2014, Revised September 15, 2014, Accepted September 22, 2014)

Abstract. This paper presents average numerical results of 2128 nonlinear dynamic finite element (FE) analyses of lightweight acceleration-sensitive non-structural components (NSCs) attached to the floors of one-bay three-storey reinforced concrete (RC) primary structures (P-structures) with different eccentricity ratios. The investigated parameters include the NSC to P-structure vibration period ratio, peak ground acceleration, P-structure eccentricity ratio, and NSC damping ratio. Appropriate constitutive relationships were used to model the behaviour of the RC P-structures. The NSCs were modelled as vertical cantilevers fixed at their bases with masses on the free ends and varying lengths so as to match the vibration periods of the P-structures. Full dynamic interaction was considered between the NSCs and P-structures. A set of seven natural bi-directional ground motions were used to evaluate the seismic response of the NSCs. The numerical results show that the acceleration response of the NSCs depends on the investigated parameters. The accelerations of the NSCs attached to the flexible sides of the P-structures increased with the increase in peak ground acceleration and P-structure eccentricity ratio but decreased with the increase in NSC damping ratio. Comparison between the FE results and Eurocode 8 (EC8) predictions suggests that, under tuned conditions, EC8 provisions underestimate the seismic response of the NSCs mounted on the flexible sides of the plan-irregular RC P-structures.

Keywords: dynamic analysis; eccentricity ratio; Eurocode 8; finite element; irregular RC buildings; non-structural components; torsion

1. Introduction

During earthquakes, the seismic response of non-structural components (NSCs) attached to the floors of irregular reinforced concrete (RC) primary structures (P-structures) can be amplified by the torsional behaviour of the P-structures (Aldeka *et al*. 2014). In irregular P-structures, the inertia

∗Corresponding author, Ph.D. Candidate, E-mail: abb037@bham.ac.uk
[a]Ph.D., Lecturer, E-mail: s.m.o.h.dirar@bham.ac.uk
[b]Professor, E-mail: a.chan@federation.edu.au
[c]Ph.D., Design Tutor, E-mail: p.vazquez@bham.ac.uk

http://www.techno-press.org/journals/eas&subpage=7 ISSN: 2092-7614 (Print), 2092-7622 (Online)

forces act on the centre of mass (CM) whereas the resisting forces of the structural elements act on the centre of rigidity (CR). Attributable to these two non-coincident forces, floor rotations that vary with time produce torsional modes in addition to the translational modes (Chandler and Hutchinson 1986). As the static eccentricity, defined as the eccentricity between the CM and CR, is the main cause of the coupling between the translational and torsional modes of irregular P-structures (De la Llera and Chopra 1994a, 1994b), it is important to study its effect on the seismic response of NSCs attached to the floors of such P-structures. Of note is that the seismic response of NSCs attached directly to the ground depends on the characteristics of the ground motion such as its frequency content. However, the behaviour of NSCs attached to the floors of an irregular RC P-structure depends on the torsional behaviour of the P-structure among other factors such as the NSC to P-structure vibration period ratio, peak ground acceleration (PGA), and the heights of the NSCs relative to that of the P-structure (Aldeka *et al*. 2014).

Research work investigating the effect of the P-structure eccentricity ratio, defined as the static eccentricity (e) divided by the elasticity radius (r), on the seismic response of NSCs is scarce. Moreover, it has produced conflicting results. For example, Agrawal and Datta carried out two analytical studies (Agrawal and Datta 1999a, 1999b) on primary-secondary (P-S) systems under tuned and un-tuned conditions. The results of the first study (Agrawal and Datta 1999a) showed that under tuned conditions the dynamic response of the NSCs increased with the increase in the P-structure eccentricity ratio ($R=e/r$) whereas an opposite trend was observed under un-tuned conditions. However, the results of the second study (Agrawal and Datta 1999b) showed that under tuned conditions the response of the NSCs decreased with the increase in the value of e/r whereas the response was almost insensitive to the change in e/r values under un-tuned conditions.

Yang and Huang (1993) investigated analytically the effect of the torsional response of a fixed base building on the seismic response of lightweight NSCs. Their approach was restricted to elastic P-S systems with classical damping and floor eccentricity in one direction only. A two-dimensional model was adopted where each storey of the building was modelled as two degrees of freedom (DOF), with one DOF for translation and the other for torsion. The results showed that the NSCs accelerations at the first translational mode of the building were higher than the corresponding values at the torsional mode.

Mohammed *et al*. (2008) studied the effect of both stiffness eccentric and mass eccentric primary systems (P-systems) on the seismic response of NSCs. The modelled P-systems, which were subjected to a unidirectional base motion, comprised a square aluminium platform (300 mm×300 mm) supported at its corners by 3 mm diameter aluminium rods with varied lengths for stiffness adjustment. The NSCs were modelled as lumped masses and were either rigid or near tuned to the fundamental vibration periods of the P-systems. The results showed that the torsional yielding of the P-systems had significant implications on the de-amplification of the seismic response of near tuned NSCs. However, Mohammed *et al*. (2008) concluded that their results were valid only for the investigated systems and cannot be generalised.

A careful evaluation of the above literature suggests that further research is needed to clarify the effect of P-structure eccentricity ratio on the seismic response of NSCs. This paper presents average numerical results of 2128 nonlinear dynamic finite element (FE) analyses of NSCs attached to the floors of RC P-structures with different eccentricity ratios. The NSCs considered in this paper are lightweight acceleration-sensitive mechanical, electrical, or medical equipment such as those found in industrial, commercial, or healthcare buildings respectively. Full dynamic interaction is considered between the P-structures and the NSCs. The main objective of this paper is to investigate the effect of NSC to P-structure vibration period ratio, peak ground acceleration,

P-structure eccentricity ratio, and NSC damping ratio on the NSCs acceleration response. This paper also evaluates the accuracy of Eurocode 8 (2004) design provisions for NSCs by comparing the average numerical results with Eurocode 8 (EC8) predictions.

2. Characteristics and modelling of the RC P-structures

Eight variants of a single-bay three-storey RC structure with different eccentricity ratios were selected as P-structures. The eccentricity ratio was varied by changing the sizes of the corner columns of the P-structures. This specific configuration was chosen as it represented the most straightforward approach to investigating the effect of P-structure eccentricity ratio on the seismic response of NSCs. Shown in Fig. 1(a) and 1(b) are the plan and elevation of the P-structures respectively. The P-structures had a 5.5 m centre-to-centre single span in both the *X* and *Y* directions (see Fig. 1(a)) and square column cross-sections.

2.1 Characteristics of the RC P-structures

Tables 1 and 2 detail the characteristics of the RC P-structures. A regular RC structure with 500 mm×500 mm column cross-sections was designed as a reference structure. For the remaining seven variants of the reference structure, the static eccentricity was varied by changing the cross-sectional dimensions of the corner columns. The column cross-sections were designed in such a way that the total lateral elastic stiffness in the horizontal directions (*X* and *Y*) was constant for each structure (see Table 2).

For each P-structure, the CM coordinates (g_x, g_y) and the CR coordinates (l_x, l_y) reported in Table 2 are measured from Point *O* at the lower left corner of Fig. 1(a).

The design of the RC P-structures in terms of the imposed loads, member resistance, and seismic resistance was carried out according to the provisions of Eurocode 1 (EC1 2002), Eurocode 2 (EC2 2004), and EC8 (2004) respectively. The characteristic values of the floor loads were taken as 2.5 kN/m^2 and 2.0 kN/m^2 for permanent (excluding slab self-weight) and variable actions respectively. The total permanent action acting on the columns at each floor level was kept constant.

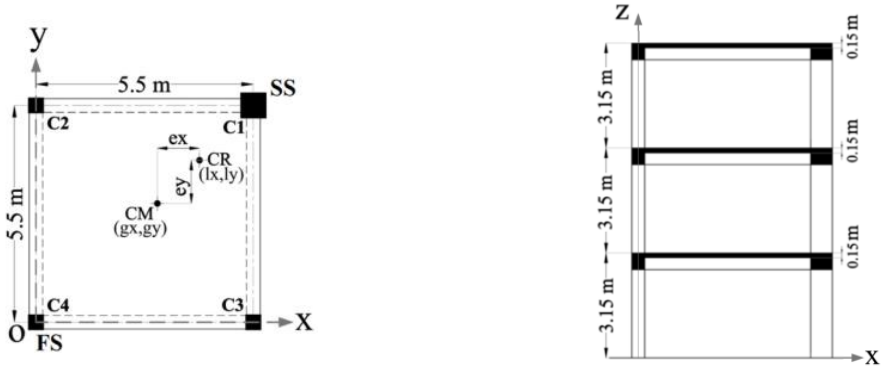

(a) (b)

Fig. 1 RC P-structures: (a) plan and (b) elevation

Table 1 Details of the column cross-sections (all dimensions in mm)

Building	Column C1				Columns C2, C3, and C4			
	Cross section	Long. steel	Shear links (critical region)	Joint shear links	Cross section	Long. steel	Shear links (critical region)	Joint shear links
Reference	500×500	12Ø 20	3Ø 8@120	3Ø 8@100	500×500	12Ø 20	3Ø 8@120	3Ø 8@90
Modified 1	525×525	12Ø 20	3Ø 8@130	3Ø 8@100	491×491	12Ø 20	3Ø 8@120	3Ø 8@90
Modified 2	550×550	14Ø 20	3Ø 8@140	3Ø 8@110	479×479	12Ø 20	3Ø 8@120	3Ø 8@90
Modified 3	575×575	16Ø 20	3Ø 8@140	3Ø 8@110	465×465	12Ø 20	3Ø 8@120	3Ø 8@90
Modified 4	600×600	16Ø 20	3Ø 8@140	3Ø 8@110	448×448	14Ø 20	3Ø 8@100	3Ø 8@90
Modified 5	625×625	18Ø 20	3Ø 8@140	3Ø 8@110	425×425	14Ø 20	3Ø 8@100	3Ø 8@90
Modified 6	650×650	20Ø 20	4Ø 8@150	4Ø 8@120	393×393	14Ø 20	3Ø 8@80	3Ø 8@70
Modified 7	675×675	22Ø 20	4Ø 8@150	4Ø 8@120	345×345	12Ø 20	2Ø 8@80	2Ø 8@70

Table 2 Eccentricity and stiffness details of the RC P-structures

Building	CM coordinates (g_x, g_y), [m]	CR coordinates (l_x, l_y), [m]	Eccentricity (e_x=e_y), [m]	Lateral stiffness (K_x=K_y), [kN/m]	Torsional stiffness (K_R), [kN.m/rad]	Elasticity radius (r_x=r_y), [m]	Eccentricity ratio (R_x=R_y)
Reference	(2.75,2.75)	(2.75,2.75)	0.00	291435	4407957	3.89	0.000
Modified 1	(2.85,2.85)	(2.95,2.95)	0.10	291435	4385210	3.88	0.026
Modified 2	(2.95,2.95)	(3.18,3.18)	0.23	291435	4302459	3.84	0.060
Modified 3	(3.07,3.07)	(3.44,3.44)	0.37	291435	4133195	3.77	0.098
Modified 4	(3.21,3.21)	(3.73,3.73)	0.52	291435	3843441	3.63	0.143
Modified 5	(3.37,3.37)	(4.07,4.07)	0.70	291435	3390371	3.41	0.205
Modified 6	(3.58,3.58)	(4.45,4.45)	0.87	291435	2720631	3.06	0.284
Modified 7	(3.88,3.88)	(4.88,4.88)	1.00	291435	2104515	2.69	0.372

The RC P-structures were designed using the EC8 (2004) type 1 spectrum for ground type C. The design ground acceleration on type A ground (a_g) was taken as 0.15 g. Considering the soil factor of 1.15 for ground type C, the design ground acceleration on type C ground was 0.173 g. The behaviour factor (q) was taken as 3.3 according to EC8 (2004) Clause 5.2.2.2. All P-structures satisfied the EC8 (2004) Ductility Class M (DCM) requirements which necessitate the use of concrete of a class higher than C16/20 and Class B or C high ductility steel reinforcement in the main structural members. Concrete Class C25/30 and steel reinforcement Class C S500 were therefore used in the design of the structural elements. To fulfil the strong column/weak beam criterion, the over-strength factor (γ_{Rd}) was taken as 1.30 for all P-structures.

2.2 Modelling of the RC P-structures

The FE code MIDAS Gen ver. 3.1 (2012) was used to perform the nonlinear dynamic analyses of the P-S systems. Validation of MIDAS Gen code for the dynamic analysis of irregular RC P-

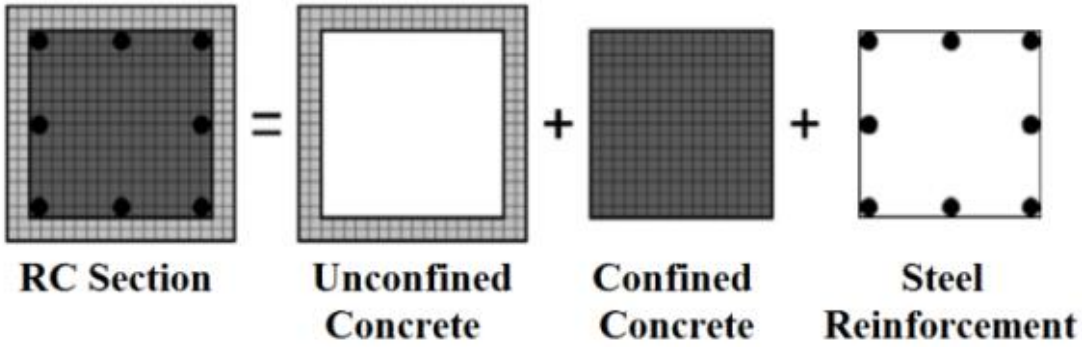

Fig. 2 Description of a reinforced concrete section as implemented in MIDAS Gen code (2012)

structures with significant torsional behaviour was reported by Aldeka *et al*. (2014).

The P-structures were modelled with a distributed inelastic fibre element as shown in Fig. 2. Confined and unconfined concrete models proposed by Mander *et al*. (1988) and the steel reinforcement model developed by Menegotto and Pinto (1973) were used to model the concrete and steel reinforcement cyclic behaviour respectively. The input parameters required to define the concrete models are the cylinder compressive strength (taken as 25 MPa) and the unconfined concrete peak strain (taken as 0.002). The concrete elastic modulus, tensile strength, and tensile strain are automatically computed by MIDAS Gen (2012). The input parameters required to define the steel reinforcement model proposed by Menegotto and Pinto (1973) are the yield strength (taken as 500 MPa), initial elastic modulus (taken as 206 GPa), and the strain hardening ratio (taken as 0.005 for ordinary steel bars). Three constants (R_o, a_1 and a_2) are required to control the transition from the elastic to the plastic branch of the steel reinforcement constitutive model. The recommended values for these constants for ordinary steel bars are 20 for R_o, 18.5 for a_1, and 0.15 for a_2 (Menegotto and Pinto 1973).

Newmark and Newton-Raphson methods were used to integrate the equations of motion and achieve convergence respectively. The values of 0.5 and 0.25 were used for Newmark's factors γ and β respectively. Based on the recommendations of Paz (1994), a damping ratio of 5% was adopted for the P-structures. Of note is that the above-mentioned material models, parameters, and solution techniques were the same as those validated by Aldeka *et al*. (2014).

2.3 Modal analysis of the RC P-structures

Modal analyses were carried out to determine the vibration periods of the P-structures (see Table 3). These analyses are essential for the selection of NSCs with vibration periods matching the vibration periods of the P-structures. It can be seen from Table 3 that the vibration periods for the translational modes (i.e., T_1, T_2, T_4 and T_5) of the P-structures are equal. This is attributable to the fact that the global lateral stiffness of the P-structures was constant (see Table 2). On the other hand, the vibration periods for the torsional modes (i.e., T_3 and T_6) increase gradually with the increase in eccentricity ratios (see Tables 2 and 3).

Figs. 3(a) and 3(b) show typical translational modes in the X and Y directions respectively whereas Fig. 3(c) shows a typical torsional mode.

Table 3 Vibration periods of the RC P-structures

Building	Vibration periods [*s*]					
	T_1	T_2	T_3	T_4	T_5	T_6
Reference	0.385	0.379	0.261	0.108	0.105	0.076
Modified 1	0.385	0.379	0.261	0.108	0.105	0.077
Modified 2	0.385	0.379	0.262	0.108	0.105	0.077
Modified 3	0.385	0.379	0.263	0.108	0.105	0.077
Modified 4	0.385	0.379	0.264	0.108	0.105	0.078
Modified 5	0.385	0.379	0.267	0.108	0.105	0.079
Modified 6	0.385	0.379	0.271	0.108	0.105	0.079
Modified 7	0.385	0.379	0.275	0.108	0.105	0.080

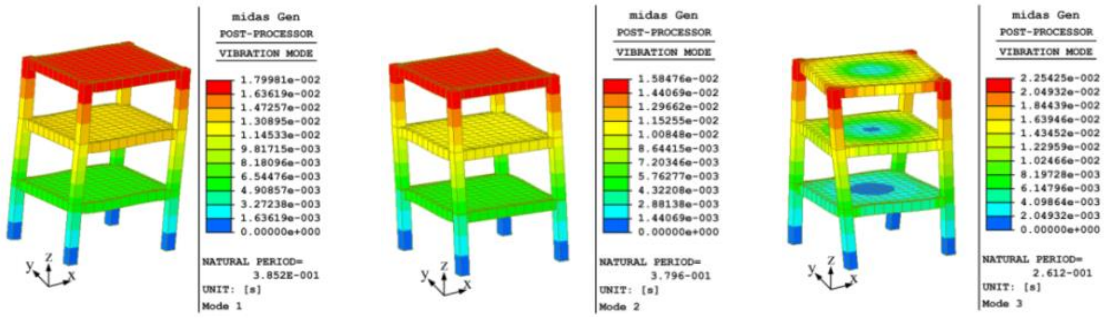

(a) (b) (c)

Fig. 3 Vibration modes: (a) translational-*X*, (b) translational-*Y* and (c) torsional

3. Non-structural components: selection, modelling, and characteristics

The NSCs considered in this paper are elastic lightweight acceleration-sensitive mechanical, electrical, or medical equipment such as those found in industrial, commercial, or healthcare buildings respectively. Normally, only the fundamental modes of such NSCs are of importance therefore they can be modelled as vertical cantilevers fixed at their bases with lumped masses on their free ends (Yang and Huang 1993, 1998, Agrawal 1999, Mohammed *et al*. 2008, Chaudhuri and Villaverde 2008, Oropeza *et al*. 2010, Aldeka *et al*. 2014). A modelling approach similar to that used by Sackman and Kelly (1979) and Aldeka *et al*. (2014) was adopted in this study where the NSCs were modelled as vertical cantilevers fixed at their bases with masses on the free ends. Each cantilever had a 152×152×51 mm^3 lumped steel mass weighing about 9.25 kg. The arms of the cantilevers were modelled as circular sections, 40 mm in diameter. The circular cross-section was favoured because it has the same lateral stiffness in any horizontal direction. The length (L_a) and lateral stiffness (K_a) values of the circular cantilever arms of the NSCs are given in Table 4. These values were chosen in such a way that the NSCs vibration periods (T_C) match the first six vibration periods (T_1, T_2, T_3, T_4, T_5 and T_6) of the P-structures. Furthermore, to study the seismic response of NSCs with long vibration periods, T_C values of $2T_1$ and $4T_1$ are also considered in this paper. Fig. 4 shows the results of the eigenvalue analyses for the NSCs with the vibration periods reported in Table 4.

Table 4 Characteristics of the NSCs

NSCs Period, [*s*]	T_C=T_1	T_C=T_2	T_C=T_3	T_C=T_4	T_C=T_5	T_C=T_6	T_C=2T_1	T_C=4T_1
	0.385	0.379	0.261	0.108	0.105	0.076	0.770	1.540
L_a, [m]	1.38	1.36	1.06	0.59	0.58	0.47	2.19	2.19
K_a, [N/m]	2438.2	2547.3	5380	31199.5	32841.2	61717.7	610.1	152.5

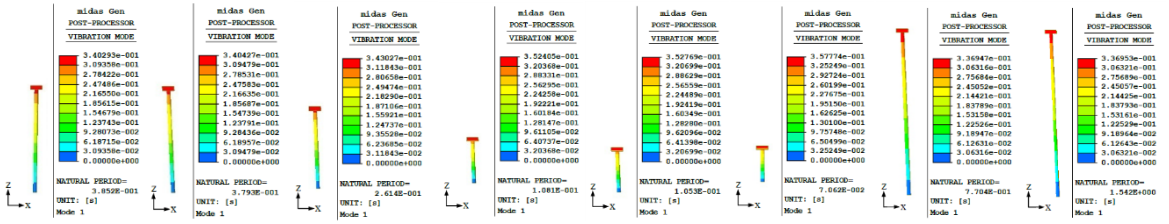

T_C=T_1 T_C=T_2 T_C=T_3 T_C=T_4 T_C=T_5 T_C=T_6 T_C=2T_1 T_C=4T_1

Fig. 4 Eigenvalue analyses of the NSCs

Full dynamic interaction is considered between the NSCs and the P-structures. Based on the recommendations of Graves and Morante (2006), a linear viscous damping ratio (ξ_c) of 3% was used for the NSCs. This damping type is adopted because NSCs do not have the same energy dissipation mechanisms as building structures. To investigate the effect of NSC damping ratio on the amplification or de-amplification in NSCs acceleration response, additional values of ξ_c equal to 0.01%, 0.2%, 0.5%, 1%, 2%, 4%, and 5% were also considered.

4. Nonlinear static (push-over) analyses of the P-structures

As will be detailed in Section 6, PGA values ranging from 0.05 g to the values corresponding to the maximum seismic capacities of the P-structures, including the PGA values corresponding to the elastic seismic capacities, were used to investigate the seismic response of the NSCs. Nonlinear static analyses were therefore carried out to evaluate the elastic and maximum seismic capacities of the RC P-structures. The displacement values at near collapse (NC) obtained from the nonlinear static analyses were corrected by considering the torsional effect using the extension of the N2 procedure (see Fig. 5). The extended N2 procedure is a simplified nonlinear method for the seismic analysis of plan-asymmetric structures. It can be used to calculate the seismic capacities and the idealised force-displacement response of such structures by combining the results obtained from push-over analysis of a three-dimensional (3D) structural model with the results of a linear dynamic analysis (Fajfar *et al*. 2005). Further details on the extended N2 procedure can be found in Kreslin and Fajfar (2010), Stefano and Pintucchi (2010).

For each P-structure, Table 5 details the characteristics of the idealised elastic-perfectly plastic force-displacement relationship determined according to Annex B of EC8 (2004). The idealised force-displacement curves were used to calculate the elastic and maximum seismic capacities of the P-structures. The initial stiffness of the idealised system is determined in such a way that the areas under the actual and idealised force-displacement curves are equal.

The characteristics detailed in Table 5 above are the maximum seismic capacity, weight (W), effective mass (m^*), transformation constant (Γ), base shear (F_y), near collapse displacement (d_m),

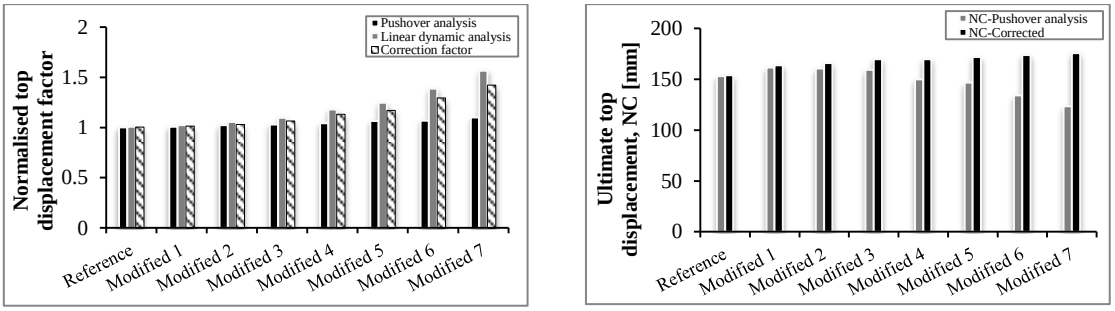

(a) (b)

Fig. 5 Push-over analyses results: (a) normalised top displacement factor and (b) corrected top displacements values at near collapse (NC)

Table 5 Maximum seismic capacities and characteristics of the idealised force-displacement relationships

Building	Max. seismic Capacity [g]	W [kN]	m^* [kg].10^3	Γ	F_y [kN]	d_m [m]	E_m [kN.m]	d_y [m]	T^* [s]	S_{ae} [g]	S_{ay} [g]	μ	d_t [m]	d_m/d_t
Reference	0.57	1632	115.0	1.27	528.9	0.154	75.5	0.023	0.44	1.44	0.37	3.91	0.149	1.03
Modified 1	0.57	1632	115.0	1.27	508.2	0.164	77.3	0.023	0.45	1.44	0.35	4.06	0.159	1.03
Modified 2	0.56	1632	115.0	1.27	506.4	0.166	77.9	0.025	0.47	1.41	0.35	3.99	0.166	1.00
Modified 3	0.55	1632	115.0	1.27	504.0	0.170	79.2	0.026	0.48	1.39	0.35	3.96	0.170	1.00
Modified 4	0.55	1632	115.0	1.27	502.5	0.170	79.0	0.026	0.48	1.39	0.35	3.96	0.170	1.00
Modified 5	0.55	1632	115.0	1.27	519.7	0.172	82.4	0.027	0.49	1.39	0.36	3.82	0.170	1.01
Modified 6	0.54	1632	115.0	1.27	519.2	0.174	83.0	0.028	0.49	1.35	0.36	3.74	0.174	1.00
Modified 7	0.54	1632	115.0	1.27	519.5	0.176	84.0	0.028	0.49	1.35	0.36	3.73	0.171	1.03

Table 6 Elastic seismic capacities of the RC P-structures

Building	Elastic seismic capacity [g]	S_{ae} [g]	S_{ay} [g]	μ
Reference	0.15	0.37	0.37	1.00
Modified 1	0.14	0.36	0.35	1.02
Modified 2	0.14	0.36	0.35	1.02
Modified 3	0.14	0.36	0.35	1.02
Modified 4	0.14	0.36	0.35	1.02
Modified 5	0.15	0.37	0.36	1.02
Modified 6	0.15	0.37	0.36	1.02
Modified 7	0.15	0.37	0.36	1.02

actual deformation energy (E_m), yield displacement (d_y), effective period of the idealised equivalent single DOF system (T^*), elastic acceleration response (S_{ae}) at T^*, acceleration at the yield point (S_{ay}), and target displacement of the multiple DOF system (d_t). It can be seen from Table 5 that the maximum seismic capacity of each P-structure is given by the PGA value corresponding to a value of d_m/d_t approximately equal to 1.0.

According to Annex B of EC8 (2004), a structure can be considered within the elastic range when its ductility factor (μ) is less than or equal to 1.0. Hence, the elastic seismic capacity may be

defined as the PGA value corresponding to μ=1.0. Table 6 gives the elastic seismic capacities of the P-structures considered in this study together with the values of the spectral accelerations S_{ae} and S_{ay}.

5. Earthquake records

EC8 (2004) (Clause 4.3.3.4.3) allows the use of the average effects of at least seven artificial, natural, or simulated earthquake records for design purposes. In order to evaluate the NSCs seismic response, a set of natural base motion records was used in this study. This set consists of seven pairs of natural earthquakes, all of which are compatible with the EC8 (2004) type 1 response spectrum for ground type C.

Table 7 summarises the main characteristics of the seven pairs of natural records. These earthquakes were extracted from the European Strong-motion Database (ESD) using the computer code REXEL ver. 3.2 (beta) (Iervolino *et al*. 2009, 2010). The mean response spectrum of the natural records selected using REXEL was not quite compatible with the EC8 (2004) type 1 spectrum for ground type C. The selected natural records were therefore modified using the computer software SeismoMatch ver. 2.1 (Seismosoft 2009) without increasing the number of motion cycles, as the case is for artificial records.

As seen in Fig. 6, the mean pseudo accelerations of the selected natural ground motions in the *X* and *Y* directions match the pseudo accelerations of the EC8 (2004) type 1 spectrum for ground type C with 5% damping. In Fig. 6, the PGA value of 1.0 g was used to scale the selected natural records.

Table 7 Characteristics of the natural ground motion records

Code	Name and Location	Station ID	Date	*Mw*	PGA-*X*, [m/s^2]	PGA-*Y*, [m/s^2]
000133	Friuli (aftershock)- Italy	ST33	15/09/1976	6.0	1.069	0.932
000333	Alkion- Greece	ST121	24/02/1981	6.6	2.257	3.036
000334	Alkion- Greece	ST122	24/02/1981	6.6	2.838	1.671
000335	Alkion- Greece	ST121	25/02/1981	6.3	1.144	1.176
000600	Umbria Marche- Italy	ST223	26/09/1997	6.0	1.685	1.041
000879	Dinar- Turkey	ST271	01/10/1995	6.4	2.674	3.131
001726	Adana- Turkey	ST549	27/06/1998	6.3	2.158	2.644

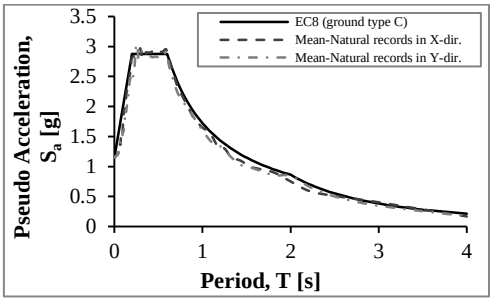

Fig. 6 Response spectra of the natural ground motions

6. Dynamic analyses of the primary-secondary systems

The results presented hereinafter are based on averages of the NSCs acceleration response to the earthquake records detailed in Section 5. Due to the 3D nature of the P-structures considered in this study, there are two peak component acceleration (PCA) values in the horizontal X and Y directions, i.e., PCA_x and PCA_y respectively. The resultant peak component acceleration (PCA_{xy}) is calculated as the square root of the sum of the squares of PCA_x and PCA_y.

In the following sections, reference will be made to the elastic and maximum seismic capacities of a given P-structure as given in Tables 6 and 5 respectively. The results presented in Sections 6.1, 6.2, and 6.3 are for NSCs with a damping ratio of 3% (based on Graves and Morante (2006)). Section 6.4 identifies the effect of NSC damping ratio on the seismic behaviour of NSCs.

6.1 Effect of NSC to P-structure vibration period ratio

The effect of NSC to P-structure vibration period ratio (T_C/T_1) on the acceleration response of the NSCs was investigated by considering different values of T_C/T_1. For NSCs attached to the flexible sides (FS) (see Fig. 1(a)) of the top floors of the P-structures, Fig. 7(a) shows the variations of PCA_{xy} with T_C/T_1 at the PGA values corresponding to the elastic seismic capacities of the P-structures whereas Fig. 7(b) presents the corresponding variations at the PGA values corresponding to the maximum seismic capacities of the P-structures. The results presented in Fig. 7 are for the NSCs attached to the FS of the top floors of the P-structures.

Similar to the findings of Aldeka *et al*. (2014), Figs. 7(a) and 7(b) show that the NSCs exhibit three zones of seismic response depending on the value of T_C/T_1. In Zone 1, NSCs accelerations increase gradually with the increase in T_C/T_1 values from 0 to 0.52. In Zone 2, the acceleration response of the NSCs increases sharply when their vibration periods match one of the first three vibration periods of the P-structures. A sharp reduction in the acceleration response of the NSCs occurs in Zone 3 for T_C/T_1 values greater than 1.0.

It can be seen from Fig. 7(a) that for $T_C=T_1$, the NSCs acceleration response increases significantly with the increase in the P-structure eccentricity ratio. For the reference P-structure (i.e., plan-regular P-structure without eccentricity), the value of PCA_{xy} was 0.83 g. However, the

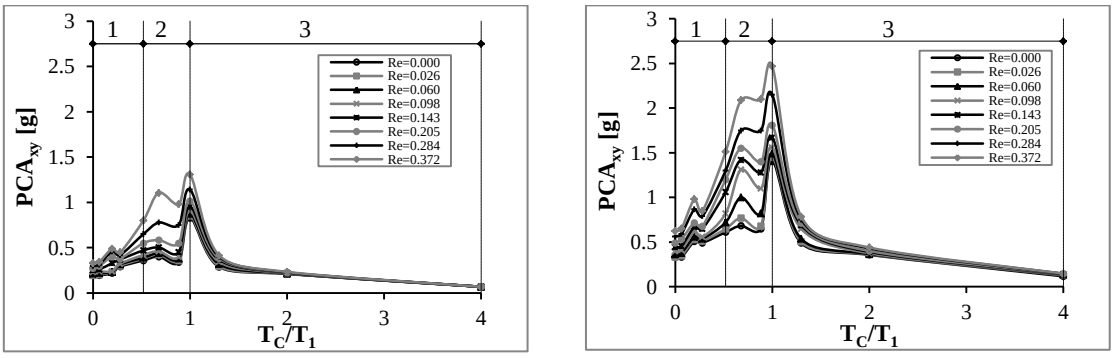

Fig. 7 Variations of peak component acceleration vs. NSC to P-structure vibration period ratio for the NSCs attached to the flexible sides of the top floors of the P-structures with different eccentricity ratios (R_e) at the PGA values corresponding to the (a) elastic and (b) maximum seismic capacities

value of PCA_{xy} was 1.31 g (i.e., 57.8% higher) for the P-structure with the eccentricity ratio of 0.372.

Fig. 7(b) shows similar trends to those depicted in Fig. 7(a). At the PGA values corresponding to the maximum seismic capacities of the P-structures (Fig. 7(b)), the NSCs with T_C=T_1 had accelerations that were on average 77% higher than the corresponding accelerations at the elastic seismic capacities of the P-structures.

6.2 Effect of peak ground acceleration

Different PGA values, ranging from 0.05 g to the PGA value corresponding to the maximum seismic capacity of each P-structure (see Table 5), were used to investigate the seismic response of the NSCs. Fig. 8 shows the variations of PCA_{xy} with PGA for the NSCs with T_C=T_1 and attached to the FS and CRs (see Fig. 1(a)) of the top floors of the P-structures.

For all considered eccentricity ratios, the FE models correctly predicted that the NSCs accelerations must vary linearly with base excitation up to the PGA values corresponding to the elastic seismic capacities of the P-structures (i.e., either 0.14 g or 0.15 g). The increase in PGA values results in a corresponding increase in the P-structures floor accelerations which, in turn, increase the NSCs accelerations. At higher PGA values, damage changes the dynamic characteristics of the P-structures and results in a non-linear relationship between NSCs accelerations and PGA. Due to torsional effects, PCA_{xy} values for the NSCs attached to the FS were higher than the corresponding values for the NSCs attached to the CRs.

Fig. 8(a) shows that the acceleration response of the NSCs attached to the FS increases with the increase in eccentricity ratio. At the PGA values corresponding to the elastic seismic capacities of the P-structures, the NSCs attached to the FS of the P-structures with the eccentricity ratios of 0.026, 0.060, 0.098, 0.143, 0.205, 0.284 and 0.372 had accelerations that were 2.7%, 5.4%, 9.3%, 15.0%, 22.6%, 37.8%, and 57.9 % higher respectively than the accelerations of the NSCs attached to the flexible side of the P-structure without eccentricity. At the PGA values corresponding to the maximum seismic capacities (see Table 5), the corresponding increases were 3.6%, 6.4%, 11.4%, 19.3%, 29.3%, 53.6%, and 76.4 % respectively.

Fig. 8(b) shows that the eccentricity ratio does not significantly affect the acceleration response of the NSCs attached to the CRs of the P-structures. The NSCs accelerations at the PGA values corresponding to the elastic seismic capacities of the P-structures were approximately equal. At the

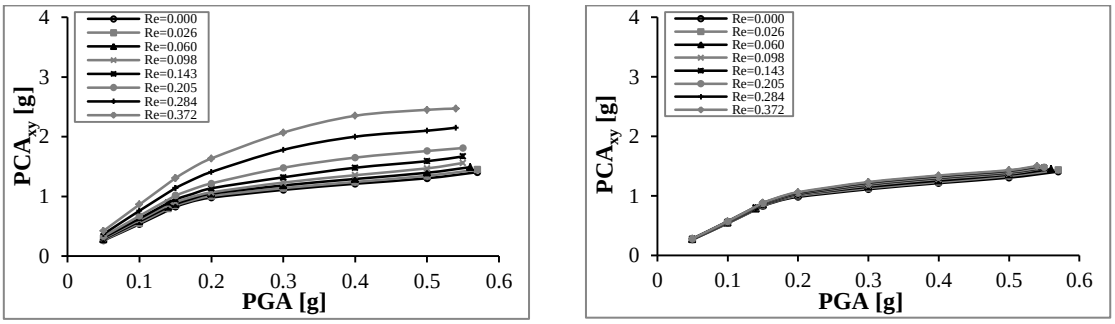

(a) (b)

Fig. 8 Variations of peak component acceleration vs. peak ground acceleration for the NSCs with T_C=T_1 and attached to the top floors of the P-structures at (a) flexible sides and (b) centres of rigidity

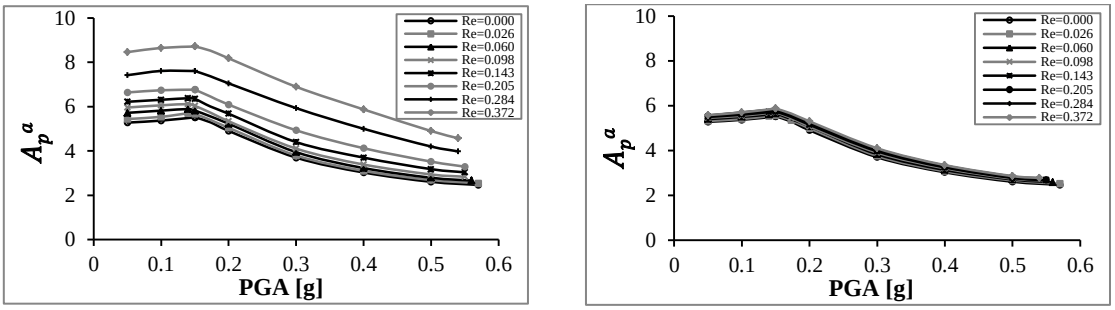

(a) (b)

Fig. 9 Variations of acceleration amplification factor vs. peak ground acceleration for the NSCs with T_C=T_1 and attached to the top floors of the P-structures at (a) flexible sides and (b) centres of rigidity

PGA values corresponding to the maximum seismic capacities, the NSCs attached to the P-structure with the highest eccentricity ratio (0.372) had accelerations that were 7% higher than the accelerations of the NSCs attached to the P-structure without eccentricity. The approximately equal accelerations at a given PGA value (see Fig. 8(b)) may be explained by the fact that the accelerations at the CRs are affected by the translational rather than the torsional characteristics of the P-structures. In this study, all P-structures had similar translational characteristics (see Tables 2 and 3).

Figs. 9(a) and 9(b) show the variations of the acceleration amplification factor (A_p^a), defined in this study as PCA_{xy}/PGA, with base excitation for the NSCs with T_C=T_1 and attached to the FS and CRs of the top floors of the P-structures respectively.

During the elastic response of the P-structures (i.e., PGA values equal to or less than the elastic seismic capacities), values of A_p^a should be constant. However, Figs. 9(a) and 9(b) show that the maximum values of the acceleration amplification factor occur at the PGA values corresponding to the elastic seismic capacities of the P-structures (see Table 6). Nonetheless, for all considered NSCs, the maximum difference in A_p^a values within the elastic range of the P-structures was less than 5.5%. The origins of this slight difference need to be further investigated. Of note is that similar results were reported by Aldeka *et al*. (2014) who argued that within the elastic range of the P-structures the NSCs accelerations vary approximately linearly with PGA. Beyond the elastic limit, the change in the dynamic characteristics of the P-structures reduces the resonance effect experienced by the NSCs. Hence, the maximum values of the acceleration amplification factor occur at the elastic seismic capacities of the P-structures.

6.3 Effect of P-structure eccentricity ratio

This section reports on the effect of P-structure eccentricity ratio on the acceleration response of NSCs with a damping ratio of 3%. Fig. 10 presents the peak component accelerations for the NSCs with T_C=T_1 and attached along the 7.78 m long diagonal line between the stiff sides (SS) and FS of the top floors of the P-structures (see Fig. 1(a)).

For a given P-structure in Fig. 10, the NSCs located between the SS and the CRs had approximately equal accelerations. Beyond the CRs, the acceleration response increased with the increase in the relative distance from the SS. This result suggests that there is no de-amplification in the acceleration response of the NSCs attached to the SS. It can also be seen in Fig. 10 that, at a

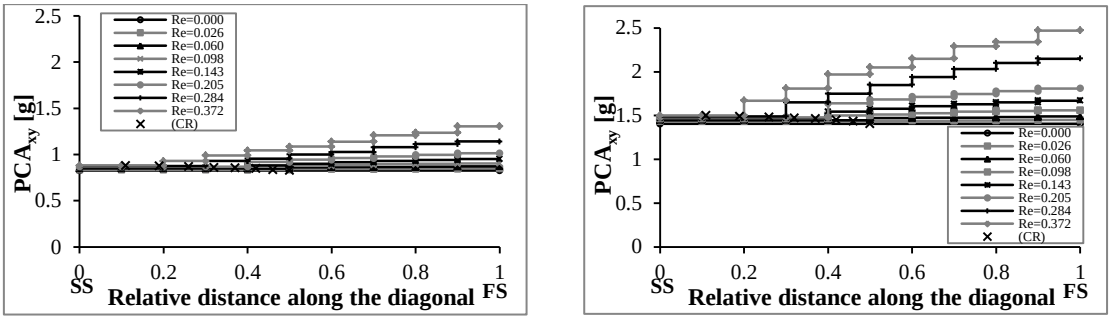

(a) (b)

Fig. 10 Peak component accelerations for the NSCs with T_C=T_1 and attached between the stiff sides and flexible sides of the top floors of the P-structures at the PGA values corresponding to (a) the elastic seismic capacities and (b) the maximum seismic capacities

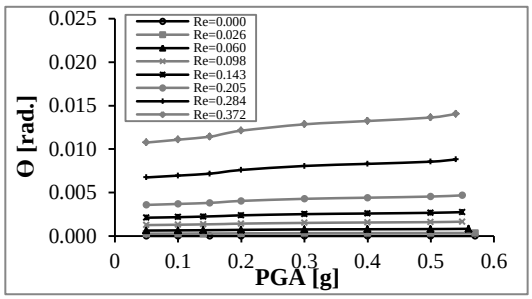

Fig. 11 Variations of top floor rotation with PGA

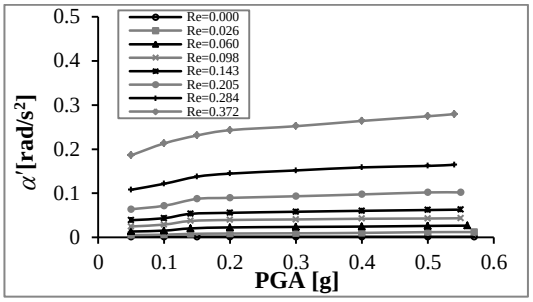

Fig. 12 Variations of top floor angular acceleration with PGA

given relative distance beyond the CRs, the acceleration response increases with the increase in the eccentricity ratio.

In this study, the torsional amplification factor (F_T) is used to quantify the relationship between the NSCs accelerations and the torsional behaviour of the P-structures caused by the eccentricity ratio. The torsional amplification factor for NSCs accelerations may be defined as the ratio of peak component acceleration at the flexible side ($PCA_{xy,FS}$) to the corresponding value at the centre of rigidity ($PCA_{xy,CR}$), i.e., (F_T=$PCA_{xy,FS}$/$PCA_{xy,CR}$) (Hart *et al*. 1975, Aldeka *et al*. 2014).

Figs. 11 and 12 show respectively the variations of top floor rotation (θ) and top floor angular acceleration (α') with PGA. These two figures show that, for a given PGA value, both θ and α' increase with the increase in the eccentricity ratio. The P-structure with the highest eccentricity ratio (0.372) experienced the highest top floor rotation (0.014 rad) and angular acceleration (0.279 rad/s^2) at the PGA value corresponding to its maximum seismic capacity (0.54 g).

Fig. 13, which depicts the variations of F_T with PGA, shows that the NSCs attached to the P-structure with the highest eccentricity ratio (0.372) had the highest torsional amplification factor (1.61). On the other hand, the P-structures with the eccentricity ratios of 0, 0.026, and 0.060 had the lowest top floor rotations (ranging from 0.00001 rad to 0.00083 rad), lowest top floor angular accelerations (ranging from 0.0015 rad/s^2 to 0.0267 rad/s^2), and lowest values of F_T (ranging from 1.0 to 1.04).

Figs. 11, 12 and 13 suggest that there is a strong correlation between F_T and θ as well as F_T and

α'. Figs. 14 and 15 show that the relationships between F_T and θ and F_T and α' may be expressed as follows

$$F_T = 45.4\theta + 1.0 \quad (1)$$

$$F_T = 2.36\alpha' + 1.0 \quad (2)$$

Solving Eqs. (1) and (2) simultaneously, the dominant frequency of rotation can be computed as $f=(45.4/2.36)^{1/2}/2\pi=0.7$ Hz. This value does not correspond to any P-structure vibration mode whereas it may correspond to dominant frequencies in ground motions for ground type C. This implies that Eqs. (1) and (2) are applicable for ground type C only. However, Eqs. (1) and (2) are valid for both regular and irregular P-structures. For a regular P-structure (e.g., the P-structure without eccentricity) that does not experience floor rotations during earthquakes, Eqs. (1) and (2) predict a torsional amplification factor of 1.0. F_T becomes greater than 1.0 when the P-structure exhibits torsional behaviour (i.e., for the P-structures with eccentricity ratios). It can be concluded that the increase in either θ or α', which are measures of the P-structure torsional behaviour, results in a corresponding increase in F_T and consequently in the accelerations of the NSCs attached to the flexible side of the P-structure. A formula comparable to Eq. (1) was reported by Aldeka *et al*. (2014) who modelled irregular RC P-structures with different heights. A maximum standard deviation of 0.026 was found between Eq. (1) above and the corresponding relationship reported by Aldeka *et al*. (2014).

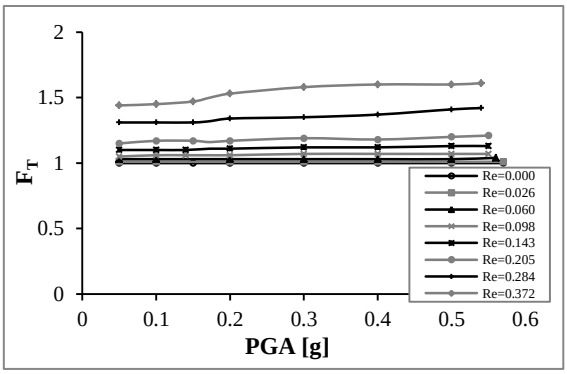

Fig. 13 Variations of torsional amplification factor for the NSCs with T_C=T_1 vs. peak ground acceleration

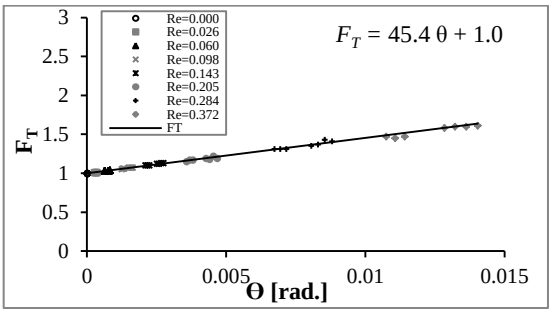

Fig. 14 Relationship between the torsional amplification factor and top floor rotation

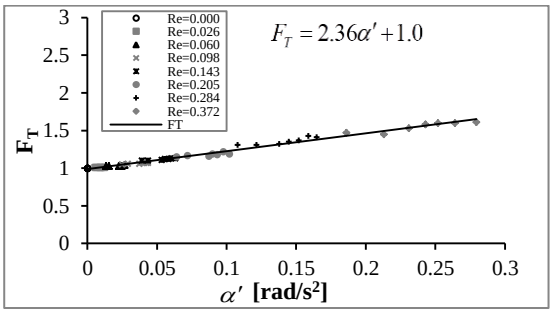

Fig. 15 Relationship between the torsional amplification factor and angular acceleration

6.4 Effect of NSC damping ratio

Evaluating the effect of NSC damping ratio is important to provide a reasonable quantification of the NSCs accelerations. NSCs damping ratios in the range between 0.01% and 5.0% were considered in this study. These values were selected based on the premise that NSCs damping ratios are, in general, much less than P-structures damping ratios.

At the PGA values corresponding to the elastic seismic capacities (either 0.14 g or 0.15 g), Figs. 16(a) and 16(b) show the variations of peak component accelerations with NSC damping ratio for the NSCs mounted on the flexible sides of the top floors of the P-structures with the lowest (0.026) and highest (0.372) eccentricity ratios respectively. It can be seen from Fig. 16 that the NSCs with vibration periods tuned to the first three vibration periods of the P-structures (i.e., T_1, T_2 and T_3) had higher accelerations than the NSCs tuned to the remaining vibration periods of the P-structures (i.e., T_4, T_5 and T_6).

The accelerations of the NSCs with T_C=T_1, T_2 or T_3 decreased with the increase in damping ratio from 0.01% to 3%. For the P-structures with the eccentricity ratios of 0.026 and 0.372, the NSCs accelerations decreased by about 40% and 48% respectively with the increase in damping ratio from 0.01% to 3%. The accelerations of the NSCs with T_C=T_4, T_5 or T_6 were less affected by the increase in damping ratio. The average percentage decrease in these NSCs accelerations ranged from 21% to 23% when the damping ratio was increased from 0.01% to 3%. At higher damping ratios (i.e., from 3% to 5%), the NSCs accelerations were not significantly affected by the increase in damping ratio.

At the PGA values corresponding to the maximum seismic capacities (either 0.57 g or 0.54 g), Figs. 17(a) and 17(b) show the variations of peak component accelerations with NSC damping ratio for the NSCs mounted on the flexible sides of the top floors of the P-structures with the lowest (0.026) and highest (0.372) eccentricity ratios respectively.

Fig. 17 features similar trends to those plotted in Fig. 16. For the P-structures with the eccentricity ratios of 0.026 and 0.372, the accelerations of the NSCs with T_C=T_1, T_2 or T_3 decreased by about 41% and 50% respectively with the increase in damping ratio from 0.01% to 3%. The accelerations of the NSCs with T_C=T_4, T_5 or T_6 were less affected by the increase in damping ratio. The average percentage decrease in these NSCs accelerations ranged from 22% to 26% when the damping ratio was increased from 0.01% to 3%. At higher damping ratios (i.e.,

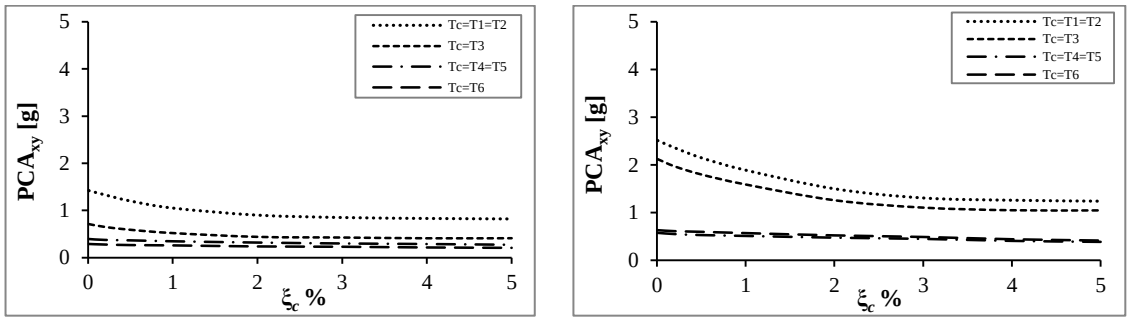

Fig. 16 Variations of peak component acceleration vs. NSC damping ratio at the PGA values corresponding to the elastic seismic capacities of the P-structures with the eccentricity ratio of: (a) 0.026 and (b) 0.372

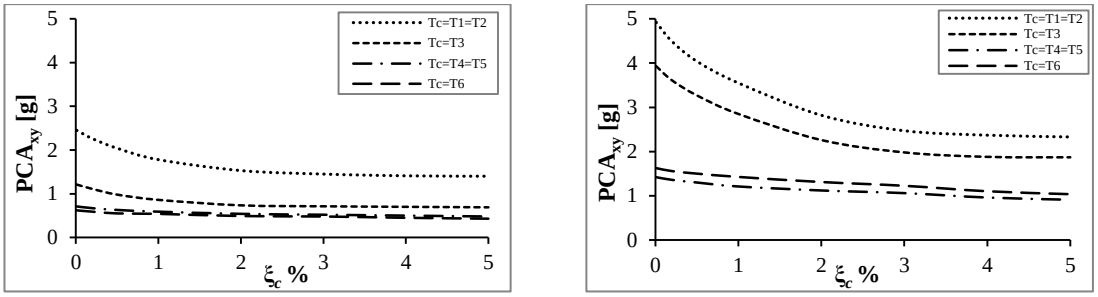

(a) (b)

Fig. 17 Variations of peak component acceleration vs. NSC damping ratio at the PGA values corresponding to the maximum seismic capacities of the P-structures with the eccentricity ratio of: (a) 0.026 and (b) 0.372

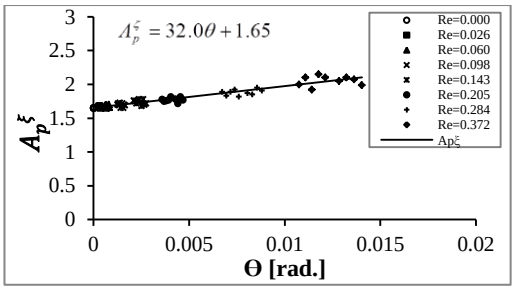

Fig. 18 Relationship between the damping amplification factor and top floor rotation

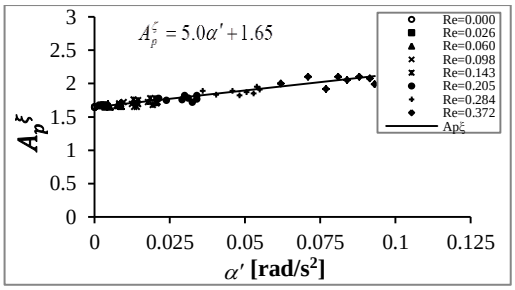

Fig. 19 Relationship between the damping amplification factor and angular acceleration

from 3% to 5%), the NSCs accelerations were not significantly affected by the increase in damping ratio.

To quantify the effect of torsion on the amplification in the accelerations of the NSCs with low damping ratios, a relationship is suggested between the damping amplification factor (A_p^{ξ}) and either the top floor rotation or the top floor angular acceleration. Figs. 18 and 19 show that the proposed relationships can be written as follows

$$A_p^{\zeta} = 32.0\theta + 1.65 \tag{3}$$

$$A_p^{\zeta} = 5.0\alpha' + 1.65 \tag{4}$$

where A_p^{ξ} is the ratio of peak component acceleration for the NSCs with 0.01% damping ratio to the peak component acceleration for the NSCs with 3% damping ratio (i.e., A_p^{ξ} = PCA$_{xy,\xi c=0.01\%}$/ PCA$_{xy,\xi c=3\%}$). Eqs. (3) and (4) show that the minimum value of A_p^{ξ} is 1.65 for the NSCs attached to the P-structure without eccentricity.

Solving Eqs. (3) and (4) simultaneously, the dominant frequency can be computed as f=(32.0/5.0)$^{1/2}$/2π=0.4 Hz. This value does not correspond to any P-structure vibration mode whereas it may correspond to dominant frequencies in ground motions for ground type C. This implies that, similar to Eqs. (1) and (2), Eqs. (3) and (4) are applicable for ground type C only.

7. Comparison between the FE results and EC8 predictions

EC8 (2004) suggests the following expression for calculating the seismic coefficient (S_a) applicable to non-structural elements

$$S_a = \alpha S \left[\frac{3[1+(z/H)]}{1+[1-(T_C/T_1)]^2} - 0.5 \right] \tag{5}$$

where

α is the ratio of the design ground acceleration on type A ground, a_g, to the acceleration of gravity;

S is the soil factor (based on EC8 (2004) Table 3.2, S is taken as 1.15 for ground type C and EC8 type 1 elastic response spectrum which are considered in this study);

T_C is the fundamental vibration period of the NSC;

T_1 is the fundamental vibration period of the building in the relevant direction;

z is the height of the NSC above the level of application of the seismic action; and

H is the building height measured from the level of application of the seismic action.

Hence, multiplying S_a, as given by Eq. (5), by the acceleration of gravity (g) yields the EC8 (2004) prediction for the design acceleration of NSCs. In order to compare the predictions of Eq. (5) with the FE results, the term αS in Eq. (5) was taken as 0.173 and the earthquake records detailed in Section 5 were scaled using the PGA value of 0.173 g (i.e., the design ground acceleration on type C ground).

Shown in Figs. 20, 21 and 22 are the comparisons between the predictions of Eq. (5) and the corresponding numerical values for different values of T_C/T_1 for the NSCs attached to the CRs and FS of the first, second, and top floors of the P-structures respectively. Good agreement can be observed in Figs. 20(a), 21(a) and 22(a) between the EC8 (2004) predictions and the numerical results for the accelerations of the NSCs with $T_C=T_1$ and attached to the CRs of the P-structures. For other values of T_C/T_1, EC8 (2004) provides conservative estimates for the accelerations of the NSCs attached to the CRs of the P-structures.

On the other hand, as can be seen in Figs. 20(b) and 21(b), EC8 (2004) underestimates the accelerations of the NSCs with $T_C=T_1$ and attached to the FS of the first and second floors of the P-structures with eccentricity ratios higher than 0.098. For the NSCs with $T_C=T_1$ and attached to the FS of the P-structures with the eccentricity ratios of 0.143, 0.205, 0.284, and 0.372; EC8 (2004)

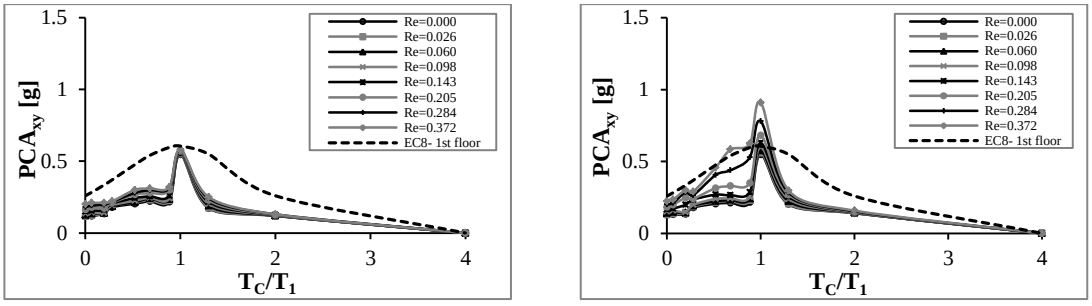

(a) (b)

Fig. 20 Comparison between FE and EC8 acceleration predictions for different values of T_C/T_1 for the NSCs attached to the first floors of the P-structures at (a) CRs and (b) FS

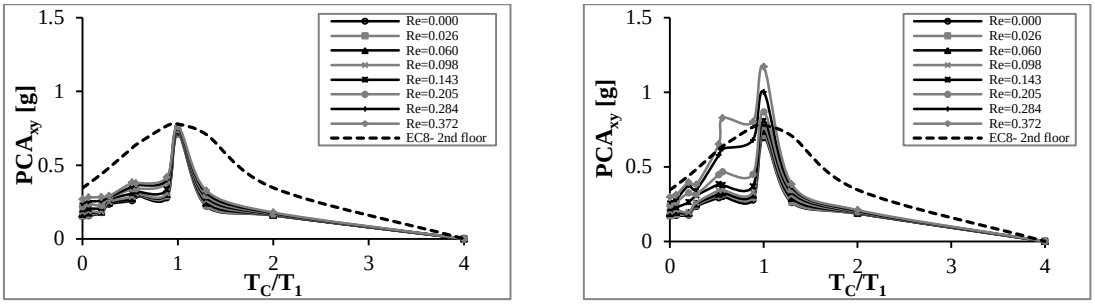

(a) (b)

Fig. 21 Comparison between FE and EC8 acceleration predictions for different values of T_C/T_1 for the NSCs attached to the second floors of the P-structures at (a) CRs and (b) FS

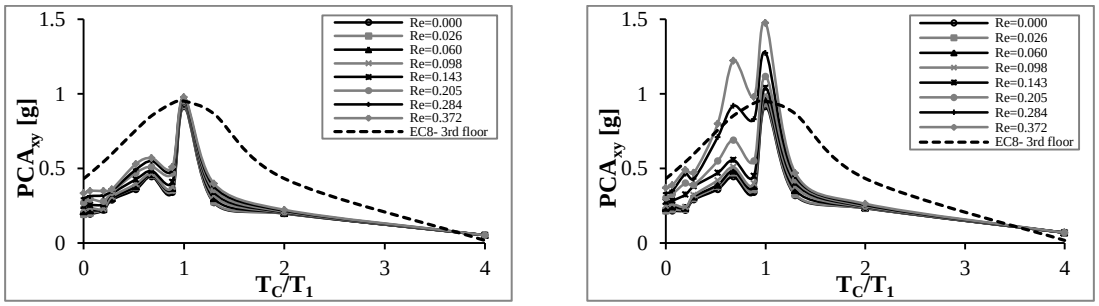

(a) (b)

Fig. 22 Comparison between FE and EC8 acceleration predictions for different values of T_C/T_1 for the NSCs attached to the third floors of the P-structures at (a) CRs and (b) FS

underestimates the acceleration response of the NSCs attached to the first floors by about 2.9%, 10.6%, 21.7%, and 33% respectively and the acceleration response of the NSCs attached to the second floors by about 3.7%, 10.3%, 22%, and 33.3% respectively.

Fig. 22(b) shows that EC8 (2004) underestimates the accelerations of the NSCs with T_C=T_1 and attached to the FS of the top floors of the P-structures with eccentricity ratios higher than 0.026. For such NSCs, EC8 (2004) underestimates the acceleration response by about 1.2%, 4.1%, 8.6%, 15%, 25.5%, and 35.6% for the NSCs attached to the P-structures with the eccentricity ratios of 0.06, 0.098, 0.143, 0.205, 0.284, and 0.372 respectively. The above results confirm previous findings (Aldeka *et al.* 2014) and contribute additional evidence suggesting that the EC8 (2004) expression for the design of NSCs, i.e., Eq. (5), needs to be modified in order to take into account the amplification in the seismic response of NSCs caused by the torsional behaviour of the P-structures. Of note is that EC8 (2004) does not explicitly consider the increase in NSCs accelerations caused by the torsional behaviour of the P-structures as can be inferred from Eq. (5).

8. Further considerations and future research

This paper focused on predicting the seismic response of NSCs attached to RC P-structures with different eccentricity ratios. Based on the results of this paper together with the findings of

Aldeka *et al*. (2014) where NSCs were attached to the floors of irregular RC P-structures with different heights (9 m, 15 m, 21 m, 30 m, 39 m and 45 m), modification of the EC8 (2004) provisions for the design of NSCs should be the subject of further research. One possible approach is to use the torsional amplification factor (see Eq. (1)) to take into account the amplification in NSCs accelerations caused by the P-structure torsional behaviour.

9. Conclusions

This paper investigates the seismic response of NSCs mounted on the floors of RC P-structures with different eccentricity ratios. Nonlinear dynamic finite element analyses were performed to evaluate the effect of NSC to P-structure vibration period ratio, peak ground acceleration, P-structure eccentricity ratio, and NSC damping ratio on the NSCs acceleration response. The numerical results show that the seismic response of the NSCs depends on the investigated variables.

The variation of the NSCs accelerations with base excitation is linear up to the PGA values corresponding to the elastic seismic capacities of the P-structures. At higher PGA values, damage changes the dynamic characteristics of the P-structures and results in a non-linear relationship between NSCs accelerations and PGA. The maximum values of the acceleration amplification factor, defined as the ratio between peak component acceleration to peak ground acceleration, occur at the PGA values corresponding to the elastic seismic capacities of the P-structures.

The accelerations of the NSCs attached to the flexible sides of the P-structures increased with the increase in P-structure eccentricity ratio. The P-structure eccentricity ratio did not significantly affect the acceleration response of the NSCs attached to the centres of rigidity of the P-structures.

The accelerations of the NSCs with vibration periods matching one of the first three vibration periods of the P-structures decreased with the increase in NSC damping ratio. The accelerations of the NSCs with vibration periods matching one of the 4^{th}, 5^{th}, or 6^{th} vibration periods of the P-structures were less affected by the increase in NSC damping ratio.

Comparison of the Eurocode 8 predictions for the design acceleration of NSCs with the corresponding numerical results suggests that, under tuned conditions, Eurocode 8 design provisions underestimate the acceleration response of the NSCs mounted on the flexible sides of the P-structures. The differences between Eurocode 8 predictions and the numerical results increased with the increase in P-structure eccentricity ratio and the height at which the NSCs were attached.

Acknowledgments

The FE analyses presented in this paper were performed using the University of Birmingham high performance computing facility (BlueBEAR). The first author acknowledges the financial support of the Iraqi Ministry of Higher Education and Scientific Research.

References

Agrawal, A.K. (1999), "Non-linear response of light equipment system in a torsional building to bi-

directional ground excitation", *Shock Vib*., **6**(5), 223-236.
Agrawal, A.K. and Datta, T. (1999a), "Seismic behavior of a secondary system on a yielding torsionally coupled primary system", *J. Seismol. Earthq. Eng.*, **2**(1), 35-46.
Agrawal, A.K. and Datta, T. (1999b), "Seismic response of a secondary system attached to a torsionally coupled primary system under bi-directional ground motion", *J. Earthq. Technol. ISET*, **36**(1), 27-42.
Aldeka, A.B., Chan, A.H.C. and Dirar, S. (2014), "Response of non-structural components mounted on irregular RC buildings: comparison between FE and EC8 predictions", *Earthq. Struct.*, **6**(4), 351-373.
Chandler, A. and Hutchinson, G. (1986), "Torsional coupling effects in the earthquake response of asymmetric buildings", *Eng. Struct*., **8**(4), 222-236.
Chaudhuri, S.R. and Villaverde, R. (2008), "Effect of building nonlinearity on seismic response of nonstructural components: a parametric study", *J. Struct. Eng*., ASCE, **134**(4), 661-670.
De la Llera, J.C. and Chopra, A.K. (1994a), "Evaluation of code accidental-torsion provisions from building records", *J. Struct. Eng*., ASCE, **120**(2), 597-616.
De la Llera, J.C. and Chopra, A.K. (1994b), *Accidental and natural torsion in earthquake response and design of buildings*, Earthquake Engineering Research Center, University of California, Berkeley, USA.
EC1 (2002), EN 1991-1-1 Eurocode 1, *Actions on structures, Part 1-1: General actions - Densities, self-weight, imposed loads for buildings*, European Committee for Standardization, Brussels, Belgium.
EC2 (2004), EN 1992-1-1 Eurocode 2, *Design of concrete structures, Part 1-1: General rules and rules for buildings*, European Committee for Standardization, Brussels, Belgium.
EC8 (2004), EN 1998-1 Eurocode 8, *Design of structures for earthquake resistance, Part 1: General rules, seismic actions and rules for buildings*, European Committee for Standardization, Brussels, Belgium.
ESD European Strong motion Database, http://www.isesd.cv.ic.ac.uk/.
Fajfar, P., Marušić, D. and Peruš, I. (2005), "Torsional effects in the pushover-based seismic analysis of buildings", *J. Earthq. Eng*., **9**(6), 831-854.
Graves, H. and Morante, R. (2006), *Recommendations for revision of seismic damping values in Regulatory Guide 1.61*, U.S. Nuclear Regulatory Commission, Office of Nuclear Regulatory Research, Washington.
Hart, G.C., Lew, M. and DiJulio, R.M. (1975), "Torsional response of high-rise buildings", *J. Struct. Div*., **101**(2), 397-416.
Iervolino, I., Maddaloni, G. and Cosenza, E. (2009), "A note on selection of time-histories for seismic analysis of bridges in Eurocode 8", *J. Earthq. Eng*., **13**, 1125-1152.
Iervolino, I., Galasso, C. and Cosenza, E. (2010), "REXEL: computer aided record selection for code-based seismic structural analysis", *Bull. Earthq. Eng*., **8**(2), 339-362.
Kreslin, M. and Fajfar, P. (2010), "Seismic evaluation of an existing complex RC building", *Bull. Earthq. Eng*., **8**(2), 363-385.
Mander, J., Priestley, M.N. and Park, R. (1988), "Theoretical stress-strain model for confined concrete", *J. Struct. Eng*., ASCE, **114**(8), 1804-1826.
Menegotto, M. and Pinto, P.E. (1973), "Method of analysis for cyclically loaded RC plane frames including changes in geometry and non-elastic behaviour of elements under combined normal force and bending", *Symposium on the Resistance and Ultimate Deformability of Structures acted on by well defined loads*, International Association for Bridge and Structural Engineering, Zurich, Switzerland.
MIDAS Gen (2012), *Analysis manual*, version 3.1, http://www.MidasUser.com/.
Mohammed, H.H., Ghobarah, A. and Aziz, T.S. (2008), "Seismic response of secondary systems supported by torsionally yielding structures", *J. Earthq. Eng*., **12**(6), 932-952.
Oropeza, M., Favez, P. and Lestuzzi, P. (2010), "Seismic response of nonstructural components in case of nonlinear structures based on floor response spectra method", *Bull. Earthq. Eng*., **8**(2), 387-400.
Paz, M. (1994), *International handbook of earthquake engineering codes, programs, and examples*, Springer.
Sackman, J.L. and Kelly, J.M. (1979), "Seismic analysis of internal equipment and components in structures", *Eng. Struct*., **1**(4), 179-190.
Seismosoft (2009), SeismoMatch version 2.1, http://www.seismosoft.com/.
Stefano, D.M. and Pintucchi, B. (2010), "Predicting torsion-induced lateral displacements for pushover

analysis: influence of torsional system characteristics", *Earthq. Eng. Struct. Dyn.*, **39**(12), 1369-1394.
Yang, Y.B. and Huang, W.H. (1993), "Seismic response of light equipment in torsional buildings", *Earthq. Eng. Struct. Dyn.*, **22**(2), 113-128.
Yang, Y.B. and Huang, W.H. (1998), "Equipment-structure interaction considering the effect of torsion and base isolation", *Earthq. Eng. Struct. Dyn.*, **27**(2), 155-171.

IT